Diazonaphthoquinone Molecular Glass Photoresists: Patterning without Chemical Amplification

Daniel Bratton,[†,‡] Ramakrishnan Ayothi,[†] Hai Deng,[§] Heidi B. Cao,[§] and Christopher K. Ober*[,†]

Department of Materials Science and Engineering, Cornell University, Ithaca, New York 14853-1501, and Intel Corporation, Hillsborough, Oregon 97124

Received December 13, 2006. Revised Manuscript Received March 28, 2007

Molecular glass photoresists have attracted increasing attention as next-generation replacements for traditional polymeric resists. Most of those reported so far have been based on a contrast generation mechanism known as chemical amplification, but increasing concerns as to the ultimate resolution obtainable by this process prompted us to investigate nonchemically amplified molecular glass resists. In this submission, we describe the synthesis of a *p*-tert-butyl calix[4]resorcinarene core functionalized with photoactive diazonapthoquinone groups (DNQ-CR). These materials are characterized using conventional wet chemistry techniques, such as NMR, and their amorphous nature was investigated via powder X-ray diffraction. Lithographic characterization using 405 nm radiation resulted in the formation of positive tone images, with both contrast and sensitivity increasing with the degree of functionalization. Exposure to electron-beam radiation resulted in the formation of negative tone images as small as 60 nm, and a probable cross-linking mechanism is discussed.

Introduction

The process of optical lithography is the backbone of the semiconductor industry and the resulting nanotechnology revolution.[1] These techniques enable the formation of micrometer-sized and in some cases nanometer-scale features of arbitrary complexity, and advances in next generation techniques such as extreme ultraviolet lithography (EUVL) or electron-beam (e-beam) lithography ensure that these methods will continue to be used for the foreseeable future.[2−4] In parallel to the research and development of novel lithographic tools, recent years have seen increasing research activity in the areas of novel resist materials. In particular, molecular glass resists have attracted much attention as possible replacements for traditional polymeric resists.[5,6] Molecular glass resists are discrete small molecules and may be made with monodisperse molecular weight distributions. They are typically designed with asymmetrical structures and bulky side groups to ensure an amorphous character.[7,8] The small size of these resists is thought to lead to a variety of advantages, including lower line edge roughness and superior component miscibility.[8] Although a wide variety of molecular glass architectures have been described,[9−23] the naturally irregular structures of calixarene derivatives have proved

* Corresponding author. Address: Cornell University, Department of Materials Science and Engineering, 310 Bard Hall, Ithaca, NY 14853. Phone: (607) 255 8417. Fax: (607) 255 2365. E-mail: cober@ccmr.cornell.edu.

† Cornell University.

‡ Present address: Melville Laboratory for Polymer Synthesis, Department of Chemistry, University of Cambridge, UK.

§ Intel Corporation.

(1) *Introduction to Microlithography*, 2nd ed.; Thompson, L. F., Willson, C. G., Bowden, M. J., Ed.; American Chemical Society: Washington, DC, 1994.
(2) Blumenstock, G. M.; Meinert, C.; Farrar, N. R.; Yen, A. *Proc. SPIE−Int. Soc. Opt. Eng.* **2005**, *5645*, 188.
(3) Cao, H. B.; Roberts, J. M.; Dalin, J.; Chandhok, M.; Meagley, R. P.; Panning, E. M.; Shell, M. K.; Rice, B. J. *Proc. SPIE−Int. Soc. Opt. Eng.* **2003**, *5039*, 484.
(4) Brainard, R. L.; Cobb, J.; Cutler, C. A. *J. Photopolym. Sci. Technol.* **2003**, *16*, 401.
(5) Shirota, Y. *J. Mater. Chem.* **2000**, *10*, 1.
(6) Shirota, Y. *J. Mater. Chem.* **2005**, *15*, 75.
(7) Alig, I.; Braun, D.; Langendorf, R.; Wirth, H. O.; Voigt, M.; Wendorff, J. H. *J. Mater. Chem.* **1998**, *8*, 847.
(8) Tsuchiya, K.; Chang, S. W.; Felix, N. M.; Ueda, M.; Ober, C. K. *J. Photopolym. Sci. Technol.* **2005**, *18*, 431.
(9) Yoshiiwa, M.; Kageyama, H.; Shirota, Y.; Wakaya, F.; Gamo, K.; Takai, M. *Appl. Phys. Lett.* **1996**, *69*, 2605.
(10) Yoshiiwa, M.; Kageyama, H.; Wakaya, F.; Takai, M.; Gamo, K.; Shirota, Y. *J. Photopolym. Sci. Technol.* **1996**, *9*, 57.
(11) Kadota, T.; Kageyama, H.; Wakaya, F.; Gamo, K.; Shirota, Y. *Chem. Lett.* **2004**, *33*, 706.
(12) Kadota, T.; Yoshiiwa, M.; Kageyama, H.; Wakaya, F.; Gamo, K.; Shirota, Y. *Proc. SPIE−Int. Soc. Opt. Eng.* **2001**, *4345*, 891.
(13) Kadota, T.; Kageyama, H.; Wakaya, F.; Gamo, K.; Shirota, Y. *Mater. Sci. Eng., C* **2001**, *C16*, 91.
(14) Kadota, T.; Kageyama, H.; Wakaya, F.; Gamo, K.; Shirota, Y. *J. Photopolym. Sci. Technol.* **1999**, *12*, 375.
(15) Fedynyshyn, T. H.; Sinta, R. F.; Pottebaum, I.; Cabral, A. *Proc. SPIE−Int. Soc. Opt. Eng.* **2005**, *5753*, 281.
(16) Trimble, A. R.; Tully, D. C.; Fréchet, J. M. J.; Medeiros, D. R.; Angelopoulos, M. *Polym. Prepr. (Am. Chem. Soc., Div. Polym. Chem.)* **2000**, *41*, 325.
(17) Tully, D. C.; Trimble, A. R.; Fréchet, J. M. J. *Adv. Mater.* (Weinheim, Germany) **2000**, *12*, 1118.
(18) Tully, D. C.; Trimble, A. R.; Fréchet, J. M. J. *Polym. Prepr. (Am. Chem. Soc., Div. Polym. Chem.)* **2000**, *41*, 142.
(19) Sooriyakumaran, R.; Truong, H.; Sundberg, L.; Morris, M.; Hinsberg, B.; Ito, H.; Allen, R.; Huang, W.-S.; Goldfarb, D.; Burns, S.; Pfeiffer, D. *J. Photopolym. Sci. Technol.* **2005**, *18*, 425.
(20) Sooriyakumaran, R.; Truong, H.; Sundberg, L.; Morris, M.; Hinsberg, B.; Ito, H.; Allen, R.; Huang, W.-S.; Goldfarb, D.; Burns, S.; Pfeiffer, D. *Proc. SPIE−Int. Soc. Opt. Eng.* **2005**, *5753*, 329.
(21) Kim, J. B.; Oh, T. H.; Kim, K. *Proc. SPIE−Int. Soc. Opt. Eng.* **2005**, *5753*, 603.
(22) Kim, J. B.; Oh, T. H.; Kwon, Y. G. *Proc. SPIE−Int. Soc. Opt. Eng.* **2002**, *4690*, 549.
(23) Kim, J. B.; Kwon, Y. G.; Yun, H. J.; Choi, J. H. *Proc. SPIE−Int. Soc. Opt. Eng.* **2002**, *4690*, 837.

10.1021/cm062967t CCC: $37.00
Published on Web 06/27/2007

Scheme 1. Functionalization of *p*-Tert-butyl-calix[4]resorcinarene with (A) DNQ 1,2-Naphthoquinone-2-diazido-4-sulfonyl Chloride (−4 DNQ) or (B) 1,2-Naphthoquinone-2-diazido-5-sulfonyl Chloride (−5 DNQ)

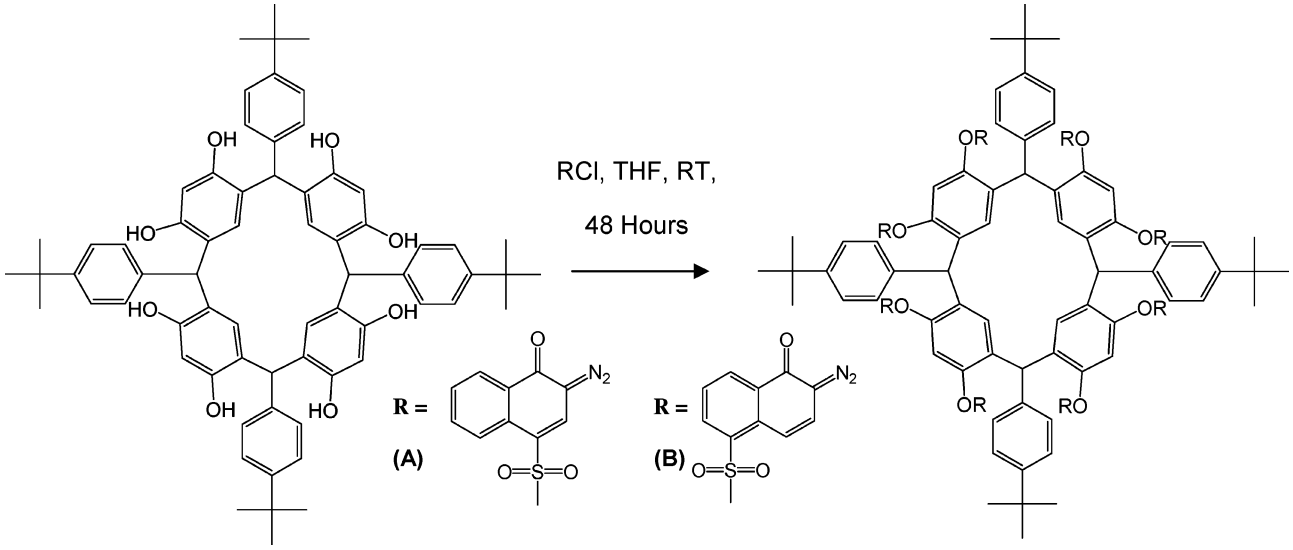

especially useful as core molecules for molecular glass resists. For example, *p*-alkylphenol calix[6] arenes,[24] *p*-chloromethyl substituted calix[4]arenes,[25] and calix[4] resorcinarenes[26−28] formulated with a suitable cross-linker have been employed a negative tone resists for e-beam and 365 nm lithography. Recently, we have reported several calix[4]arene and calix[4]resorcinarene derivatives that act as positive tone molecular glass resists for EUVL and e-beam lithography and form images as small as 30 nm.[8,29−31]

Most molecular glass resists described to date generate contrast upon exposure to radiation using a process known as chemical amplification.[32] In this process, a catalytic amount of a material known as a photoacid generator (PAG) is mixed into a formulation together with a resist comprising acidic groups (i.e., phenol or carboxylic acids) protected with acid labile functional groups (i.e., tert-butoxyl groups). Exposure to an appropriate form of radiation generates protons, which diffuse through the resist and catalyze a deprotection reaction, resulting in the exposed regions in a solubility switch from insoluble to soluble in aqueous base. Although this process leads to high sensitivity, there is increasing concern that at small feature sizes (<25 nm), the diffusion of protons from the exposed regions into the unexposed regions result in an ultimate resolution limit for chemically amplified systems.[33−35] A possible solution is to use nonchemically amplified systems, based on either chain scission resists (i.e., PMMA)[1] or photoactive compounds, which convert into a base soluble group upon exposure to radiation (e.g., diazonaphthoquinone, DNQ). Nonchemically amplified molecular glass resists have been previously reported,[9] but most are based on chain scission processes that result in high levels of outgassing, a problem for next-generation lithographic techniques.[4] Amorphous calix[8]-arenes have been blended with DNQ dissolution inhibitors to produce a positive tone image using 248 nm radiation.[36] However, no one has yet reported a base developable molecular glass resist directly functionalized with photoactive side groups, or evaluated such a compound using next-generation lithography. Such an approach could produce a single-component resist with high loadings of photoactive compounds, resulting in higher sensitivity to radiation.

In this submission, we report the synthesis and lithographic characterization of DNQ-CR, a calix[4]resorcinarene-based molecular glass resist functionalized with varying amounts of bulky DNQ side groups (Scheme 1).

We first characterize the amorphous nature of this series of resists together with the chemical changes it undergoes upon exposure to radiation. The effect of varying degrees of functionalization on sensitivity and contrast are described, along with lithographic evaluation using e-beam lithography.

Experimental Section

Materials. Resorcinol (99%), 4-tert butyl benzaldehyde (99%), anhydrous triethylamine (99.9%), and anhydrous THF were obtained from Aldrich and used as received. 1,2-Naphthoquinone-2-diazido-4-sulfonyl chloride (DNQ-Cl) and 1,2-Naphthoquinone-2-diazido-5-sulfonyl chloride were obtained from TCI America and Wako Chemicals, respectively, and both were used as received. All other organic solvents were obtained from Acros and used as received unless otherwise stated. Poly(hydroxy styrene) (MW ≈

(24) Fujita, J.; Ohnishi, Y.; Ochiai, Y.; Matsui, S. *Appl. Phys. Lett.* **1996**, *68*, 1297.
(25) Ishida, M.; Fujita, J.-i.; Ogura, T.; Ochiai, Y.; Ohshima, E.; Momoda, J. *Jpn. J. Appl. Phys., Part 1* **2003**, *42*, 3913.
(26) Haba, O.; Haga, K.; Ueda, M.; Morikawa, O.; Konishi, H. *Chem. Mater.* **1999**, *11*, 427.
(27) Nakayama, T.; Haga, K.; Haba, O.; Ueda, M. *Chem. Lett.* **1997**, *3*, 265.
(28) Nakayama, T.; Nomura, M.; Haga, K.; Ueda, M. *Bull. Chem. Soc. Jpn.* **1998**, *71*, 2979.
(29) Chang, S. W.; Felix, N.; Yang, D.; Ramakrishnan, A.; Ober, C. K. *PMSE Prepr.* **2005**, *92*, 131.
(30) Chang, S. W.; Ayothi, R.; Bratton, D.; Yang, D.; Felix, N.; Cao, H. B.; Deng, H.; Ober, C. K. *J. Mater. Chem.* **2006**, *16*, *1470.*
(31) Yang, D.; Chang, S. W.; Ober, C. K. *J. Mater. Chem.* **2006**, *16*, 1693.
(32) Reichmanis, E.; Houlihan, F. M.; Nalamasu, O.; Neenan, T. X. *Chem. Mater.* **1991**, *3*, 394.
(33) Van Steenwinckel, D.; Lammers, J. H.; Leunissen, L. H. A.; Kwinten, J. A. J. M. *Proc. SPIE−Int. Soc. Opt. Eng.* **2005**, *5753*, 269.
(34) Gallatin, G. M. *Proc. SPIE−Int. Soc. Opt. Eng.* **2005**, *5754*, 38.
(35) Schmid, G. M.; Stewart, M. D.; Wang, C.-Y.; Vogt, B. D.; Prabhu, V. M.; Lin, E. K.; Willson, C. G. *Proc. SPIE−Int. Soc. Opt. Eng.* **2004**, *5376*, 333.
(36) Nakayama, T.; Ueda, M. *J. Mater. Chem.* **1999**, *9*, 697.

20 K) used as a standard during etching studies was obtained from Aldrich and used as received.

Equipment. ^{1}H (300 MHz) and ^{13}C (76 MHz) nuclear magnetic resonance (NMR) spectra were recorded on a Bruker Advance 360 spectrometer. FTIR were obtained on a Mattson Instruments Galaxy 2020 FTIR. Thermogravimetric analysis (TGA) was carried out under nitrogen using a TA 500, and DSC data were collected with a TA 1000 using a heating rate of 10 °C min^{-1}. T_g was calculated from the second heating/cooling cycle. Powder X-ray diffraction (PXRD) traces were obtained using a Scintag Theta−Theta XDS2000 diffractometer. For lithographic evaluation, the resists were dissolved in propylene glycol monomethyl ether acetate (PGMEA, 10% solution), spin-coated at 2000 rpm for 30 s onto 4 in. silicon wafers vapor primed with hexamethyldisilazane (HMDS), and then baked at 115 °C for 2 min. After exposure, the images were developed by immersion in 0.26 N tetramethyl ammonium hydroxide (TMAH) for 30 s. Flood exposure was performed using a hand-held UV−vis lamp (E @ 366 nm = 1.35 mW/cm^2). Contrast curves were obtained at 405 nm (E = 17.8 mW/cm^2) using an HTG contact aligner. Film thickness was measured using a Tencor P10 profilometer. Exposure to e-beam was accomplished using a Leica VB6 with a tip current of 100 keV. SEM images were obtained with a Leo 982 GEMINI SEM. Etch data was obtained using an Oxford 80 RIE and compared to PHS as a standard.

Synthesis of *p*-tert-Butyl Calix[4] resorcinarene. In an adaptation of the synthesis reported by Tunstad et al.,[37] resorcinol (10 g, 0.09 mols) and 4-tert-butyl benzaldehyde (14.85 g, 0.09 mols) were dissolved in ethanol (70 mL). HCl (7.5 mL) was added, and the mixture was refluxed at 80 °C for 18 h. After being cooled to room temperature, the precipitate was filtered and washed with copious amounts of water and ethanol. The resulting white powder was dried at 60 °C overnight under reduced pressure (71% yield).

Synthesis of DNQ-Functionalized *p*-tert-Butyl Calix[4]-resorcinarene (DNQ-CR) (compound 8). As depicted in Scheme 1, *p*-tert-butyl calix[4] resorcinarene (1 g, 0.00126 mols) and triethylamine (1.25 mL, 0.01 mols) were dissolved in 30 mL of anhydrous THF under an N_2 atmosphere. 1,2-Naphthoquinone-2-diazido-4-sulfonyl chloride (2.7 g, 0.01 mols) was dissolved in a further 40 mL of anhydrous THF and added dropwise to the flask via a dropping funnel. A vigorous reaction began immediately, resulting in the evolution of gaseous HCl. After stirring at room temperature for 48 h, the contents of the flask was poured into a 4-fold excess of distilled water. The resulting brown precipitate was collected by vacuum filtration and washed with 50 mL of fresh water, and then dried overnight at 60 °C under reduced pressure (2.8 g, 76%). This basic procedure was repeated with appropriate variations in the molar quantities of DNQ-Cl and triethylamine to produce the full range of compounds with varying degrees of functionalization. The synthesis of the −5 DNQ-substituted analogue (compound 9) was accomplished in a manner analagous to the synthesis of the −4-functionalized analogues described above, employing an appropriate amount of 1,2-naphthoquinone-2-diazido-5-sulfonyl chloride.

Characterization. *Compound A (p-tert-butyl calix[4]resorcinarene).* White powder, 71% yield. ^{1}H NMR ($CDCl_3$,δ): 1.36 ($C(CH_3)_3$, 36H, s); 5.33 (CH, bridge, 4H, s); 5.97 (CH, aromatic, 4H, s); 6.52 (CH, aromatic, 4H, s); 6.96 (CH aromatic, 8H, d); 4.2 (OH, br). ^{13}C NMR ($CDCl_3$, δ): 23.2, 31.4, 40.7, 104.5, 123.3, 125.6, 127.9, 132.1, 140.3, 154.3. FTIR (NaCl plates, ν): 3480, 2962, 1608, 1496, 1074 cm^{-1}. Elemental anal. Calcd: C, 80.3. Found: C, 79.2.

(37) Tunstad, L. M.; Tucker, J. A.; Dalcanale, E.; Weiser, J.; Bryant, J. A.; Sherman, J. C.; Helgeson, R. C.; Knobler, C. B.; Cram, D. J. *J. Org. Chem.* **1989**, *54*, 1305.

Compound 1 (DNQ-CR, 12.5% average functionalized). Brown powder, 64% yield. ^{1}H NMR ($CDCl_3$, δ): 1.35 ($C(CH_3)_3$, 36H, s); 5.37 (CH, bridge, 4H, s); 5.97 (CH, aromatic, 4H, s); 6.42 (CH adjacent to azo, DNQ, 1H, s); 6.52 (CH, aromatic, 4H, s); 7.02 (CH aromatic, 8H, d); 7.33 (CH, aromatic DNQ, 1H, t); 7.51 (CH aromatic, DNQ, 2H, br); 7.78 (CH aromatic, DNQ, 1H, d), 4.8 (OH, br). ^{13}C NMR ($CDCl_3$, δ): 189, 152.8, 146.3, 143.6, 139.3, 136.8, 128.9, 124.6, 111.4, 42.7, 31.5, 26.5. FTIR (NaCl, ν): 3348, 2152, 1602, 1505, 1440, 1359, 1202, 1050 cm^{-1}. Elemental anal. Calcd: C, 74.9; N, 2.2. Found: C, 71.2; N, 2.6.

Compound 2 (DNQ-CR, 25% average functionalized). Brown powder, 61% yield. ^{1}H NMR ($CDCl_3$, δ): 1.35 ($C(CH_3)_3$, 36H, s); 5.37 (CH, bridge, 4H, s); 5.97 (CH, aromatic, 4H, s); 6.42 (CH adjacent to azo, DNQ, 2H, s); 6.52 (CH, aromatic, 4H, s); 7.02 (CH aromatic, 8H, d); 7.33 (CH, aromatic DNQ, 2H, t); 7.51 (CH aromatic, DNQ, 2H, br); 7.78 (CH aromatic, DNQ, 2H, d), 5.1 (OH, br). ^{13}C NMR ($CDCl_3$, δ): 192.4, 152.2, 146.3, 148.6, 143.3, 137.8, 127.2, 125.6, 114.4, 39.7, 33.5, 26.9. FTIR (NaCl, ν): 3351, 2146, 1605, 1506, 1437, 1362, 1210, 1045 cm^{-1}. Elemental anal. Calcd: C, 71.3; N, 3.8. Found: C, 69.2; N, 3.4.

Compound 3 (DNQ-CR, 37.5% average functionalized). Brown powder, 59% yield. ^{1}H NMR ($CDCl_3$, δ): 1.35 ($C(CH_3)_3$, 36H, s); 5.37 (CH, bridge, 4H, s); 5.97 (CH, aromatic, 4H, s); 6.42 (CH adjacent to azo, DNQ, 3H, s); 6.52 (CH, aromatic, 4H, s); 7.02 (CH aromatic, 8H, d); 7.33 (CH, aromatic DNQ, 3H, t); 7.51 (CH aromatic, DNQ, 6H, br); 7.78 (CH aromatic, DNQ, 3H, d), 3.2 (OH, br). ^{13}C NMR ($CDCl_3$, δ): 193, 153.8, 146.3, 147.6, 141.3, 136.8, 127.9, 126.6, 114.4, 41.7, 32.5, 24.5. FTIR (NaCl, ν): 3351, 2143, 1599, 1505, 1438, 1367, 1202, 1048 cm^{-1}. Elemental anal. Calcd: C, 68.7; N, 4.9. Found: C, 71.2; N, 5.4.

Compound 4 (DNQ-CR, 50% average functionalized). Brown powder, 62% yield. ^{1}H NMR ($CDCl_3$, δ): 1.35 ($C(CH_3)_3$, 36H, s); 5.38 (CH, bridge, 4H, s); 5.97 (CH, aromatic, 4H, s); 6.42 (CH adjacent to azo, DNQ, 4H, s); 6.52 (CH, aromatic, 4H, s); 7.02 (CH aromatic, 8H, d); 7.32 (CH, aromatic DNQ, 4H, t); 7.50 (CH aromatic, DNQ, 8H, br); 7.80 (CH aromatic, DNQ, 4H, d), 4.2 (OH, br). ^{13}C NMR ($CDCl_3$, δ): 189.2, 153.8, 144.3, 142.6, 140.7, 137.8, 129.3, 126.6, 111.4, 44.7, 29.5, 25.5. FTIR (NaCl, ν): 3362, 2148, 1600, 1507, 1436, 1362, 1202 and 1050 cm^{-1}. Elemental anal. Calcd: C, 66.58; N, 5.75. Found: C, 64.2; N, 6.03.

Compound 5 (DNQ-CR, 62.5% average functionalized). Brown powder, 72% yield. ^{1}H NMR ($CDCl_3$, δ): 1.35 ($C(CH_3)_3$, 36H, d); 5.37 (CH, bridge, 4H, s); 5.97 (CH, aromatic, 4H, s); 6.42 (CH adjacent to azo, DNQ, 5H, s); 6.52 (CH, aromatic, 4H, s); 7.02 (CH aromatic, 8H, d); 7.33 (CH, aromatic DNQ, 5H, t); 7.51 (CH aromatic, DNQ, 10H, br); 7.78 (CH aromatic, DNQ, 5H, d); 4.8 (OH, br). ^{13}C NMR ($CDCl_3$, δ): 191.2, 151.8, 143.3, 146.6, 140.9, 137.8, 126.3, 125.5, 113.4, 42.7, 31.5, 24.4. FTIR (NaCl, ν): 3368, 2150, 1599, 1506, 1437, 1362, 1204, 1050 cm^{-1}. Elemental anal. Calcd: C, 65.1; N, 6.43. Found: C, 71.2; N, 7.2.

Compound 6 (DNQ-CR, 75% average functionalized). Brown powder, 64% yield. ^{1}H NMR ($CDCl_3$, δ): 1.35 ($C(CH_3)_3$, 36H, s); 5.37 (CH, bridge, 4H, s); 5.97 (CH, aromatic, 4H, s); 6.42 (CH adjacent to azo, DNQ, 6H, s); 6.52 (CH, aromatic, 4H, s); 7.02 (CH aromatic, 8H, d); 7.33 (CH, aromatic DNQ, 6H, t); 7.51 (CH aromatic, DNQ, 12H, br); 7.78 (CH aromatic, DNQ, 6H, d). ^{13}C NMR ($CDCl_3$, δ): 196.2, 150.1, 144.3, 146.6, 139.3, 135.8, 128.9, 125.3, 113.4, 42.5, 32.5, 24.5 ppm. FTIR (NaCl): 3362, 2148, 1600, 1503, 1438, 1362, 1204, 1050 cm^{-1}. Elemental anal. Calcd: C, 63.8; N, 6.9. Found: C, 61.3; N, 7.6.

Compound 7 (DNQ-CR, 87.5% average functionalized). Brown powder, 69% yield. ^{1}H NMR ($CDCl_3$, δ): 1.35 ($C(CH_3)_3$, 36H, s); 5.35 (CH, bridge, 4H, s); 5.99 (CH, aromatic, 4H, s); 6.42 (CH adjacent to azo, DNQ, 7H, s); 6.52 (CH, aromatic, 4H, s); 7.02

(CH aromatic, 8H, d); 7.33 (CH, aromatic DNQ, 7H, t); 7.51 (CH aromatic, DNQ, 14H, br); 7.78 (CH aromatic, DNQ, 7H, d). ^{13}C NMR ($CDCl_3$, δ): 191.4, 151.8, 144.3, 148.6, 139.3, 135.7, 128.6, 125.2, 110.4, 42.8, 32.5, 28.5. FTIR (NaCl, ν): 3368, 2152, 1605, 1507, 1440, 1363, 1201, 1051 cm^{-1}. Elemental anal. Calcd: C, 62.9; N, 7.4. Found: C, 65.1; N, 8.9.

Compound 8 (DNQ-CR, 100% functionalized). Brown powder, 76% yield. ^{1}H NMR ($CDCl_3$, δ): 1.35 ($C(CH_3)_3$, 36H, s); 5.37 (CH, bridge, 4H, s); 5.97 (CH, aromatic, 4H, s); 6.41 (CH adjacent to azo, DNQ, 8H, s); 6.52 (CH, aromatic, 4H, s); 7.02 (CH aromatic, 8H, d); 7.33 (CH, aromatic DNQ, 8H, t); 7.51 (CH aromatic, DNQ, 16H, br); 7.78 (CH aromatic, DNQ, 8H, d). ^{13}C NMR ($CDCl_3$, δ): 193.6, 152.8, 146.3, 147.6, 140.3, 136.8, 127.9, 125.6, 112.4, 42.7, 31.5, 26.5. FTIR (NaCl, ν): 3370, 2148, 1600, 1504, 1434, 1362, 1202, 1050 cm^{-1}. Elemental anal. Calcd: C, 61. 8; N, 7.79. Found: C, 62.3; N, 6.2.

Compound 9 (5 DNQ-CR, 100% functionalized, −5-substituted analogue). Yellow powder, 68% yield. ^{1}H NMR ($CDCl_3$, δ): 1.35 ($C(CH_3)_3$, 36H, s); 5.3 (CH, alkene adjacent to azo, 8H, d); 5.38 (CH, bridge, 4H, s); 5.92 (CH, aromatic, 4H, s); 6.47 (CH, aromatic, 4H, s); 6.98 (CH aromatic, 12H, br); 7.14 (CH aromatic, 8H, d); 7.62 (CH aromatic, 8H, d); 7.75 (CH aromatic, 8H, d); 8.05 (CH aromatic, 8H, d). ^{13}C NMR ($CDCl_3$, δ): 192.2, 151.6, 147.7, 144.2, 140.2, 128.9, 125.3, 121.4, 114.6, 43.2, 32.4 ppm. FTIR (NaCl): 3369, 2147, 1601, 1499, 1432, 1363, 1202, 1050 cm^{-1}. Elemental anal. Calcd: C, 74.9; N, 2.2. Found: C, 75.6; N, 1.8.

Results and Discussion

Synthesis of DNQ-CR. The core molecule employed in this study, *p*-tert-butyl calix[4]resorcinarene, was synthesized in good yield via an acid-catalyzed condensation of *p*-tert-butyl benzaldehyde with resorcinol. The core compound is soluble in a variety of common organic solvents, and synthesis of the functionalized DNQ-CR cores was achieved using a simple substitution reaction employing triethylamine as a base. This resulted in a series of compounds functionalized with between one −4-substituted DNQ side group (compound 1, 12.5% average functionalization) to eight side groups (compound 8, 100% functionalization). Synthesis of the −5-substituted version (compound 9) was accomplished in an analogous manner. The degree of functionalization was assessed using CHN analysis and ^{1}H NMR. It was found that the average degree of functionalization matched the ratio of reactants in the feedstock.

Characterization of DNQ-CR Molecular Glass Resists. TGA showed that all samples began to decompose around 120 °C, regardless of the degree of functionalization. This corresponds to the decomposition of the azo group common to each resist. Samples 1−8, functionalized with −4 DNQ, exhibited a complex decomposition trace consistent with that previously observed for −4 DNQ esters.[38] Compound 9, functionalized with −5 DNQ, exhibited a two-stage decomposition process due to the decomposition of the DNQ group and the calix[4]resorcinarene core. Again, this decomposition is consistent with that previously observed for other DNQ esters.[38] DSC analysis showed no visible T_g. Presumably, the bulky nature of the DNQ end groups hinders molecular motion in the bulk. The amorphous character of the resist

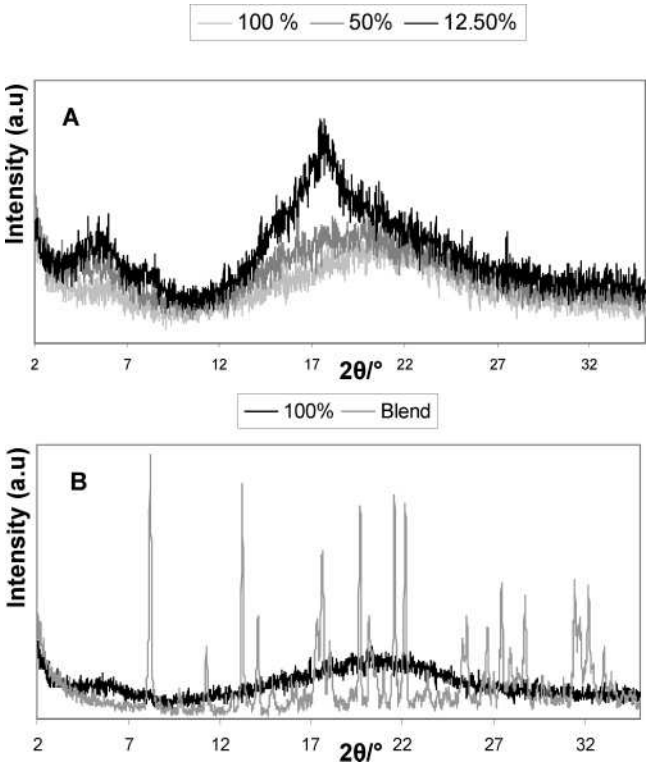

Figure 1. (A) Powder XRD traces of DNQ-functionalized calix[4]-resorcinarenes. Note how the degree of disorder in the sample increases as the degree of functionalization increases from 12.5 to 50 and through to 100%, presumably as hydrogen bonding increases. (B) Powder XRD traces illustrating that an amorphous compound is formed when the core is functionalized, as opposed to the mixture of crystalline compounds that results from simple blending.

was characterized using PXRD. The results are shown in Figure 1A. Note that only the traces from compounds 1, 4, and 8 are shown for clarity. At 100% functionalization, only broad amorphous peaks are observed, visible around 21°. As the degree of functionalization decreases, the broad peak begins to narrow and sharpen, indicating an increasing degree of order in the sample and an increase in crystallinity. This is most likely a function of increased hydrogen bonding in the samples as the degree of functionalization is decreased. However, it is clear that the functionalization of the calix-[4]resorcinarene core with bulky DNQ groups results in an amorphous resist.

DNQ photoactive compounds are usually blended with polymeric resins in order to form a working photoresist. A sample of unfunctionalized calix[4]resorcinarene was blended with DNQ in appropriate amounts to mimic the 100% functionalized system. The XRD trace of that blend (Figure 1B) consisted of separate crystalline components, quite unsuitable for spin-coating, rather than an amorphous photoresist. It is therefore apparent that the molecular glass core must be functionalized with DNQ end-groups to achieve high loadings of photoactive components, rather than simply blended.

Characterization of the Photoactive Properties of DNQ-CR. FTIR revealed that all compounds exhibited a peak around 2148 cm^{-1}, indicative of the diazido group of DNQ. After irradiation of the compounds in air with 366 nm UV radiation for 2 min, this peak disappeared to be replaced by a new peak around 1715 cm^{-1}, suggesting that the diazido

(38) Urano, Y.; Miyazaki, M.; Katsuya, K.; Kikuchi, H. *J. Photopolym. Sci. Technol.* **1993**, *6*, 53.

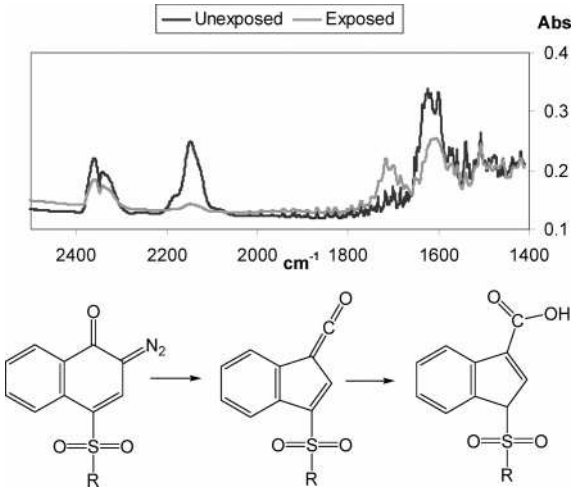

Figure 2. FTIR spectra before and after exposure to 366 nm UV radiation of a thin film of compound 8, solvent cast onto NaCl plates. Only the region from 2500 to 1400 cm^{-1} is shown. Note that after exposure, the diazo peak at 2148 cm^{-1} disappears, whereas a new peak forms at 1715 cm^{-1}, indicating the presence of a carboxylic acid. This suggests the resist undergoes the Wolff rearrangement after exposure, resulting in a solubility switch.

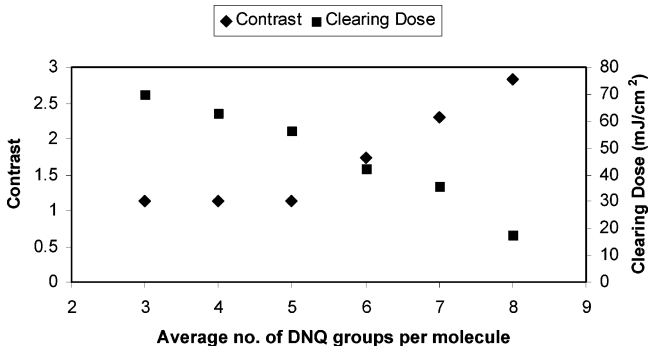

Figure 3. Influence of degree of functionality (number of DNQ groups per molecule) on clearing dose and contrast after exposure to 405 nm UV radiation, followed by development by immersion for 30 s in 0.26 N TMAH. Notice how the clearing dose is reduced with increasing DNQ, whereas contrast increases.

group was replaced by an indene carboxylic acid via the Wolff rearrangement.[1] This is demonstrated in Figure 2 using compound 8 as an illustrative example. These compounds are therefore capable of undergoing this vital conversion between the base-insoluble diazido group, to a base-soluble indene carboxylic acid group after irradiation, presumably through a ketene intermediate. The high reactivity of this species meant that we were unable to observe it directly.

Lithographic Evaluation: Contrast and Sensitivity. For an initial evaluation of lithographic performance, each sample was dissolved into a 10 w/w % solution in PGMEA, spin-coated at 2000 rpm for 30 s onto an HMDS primed wafer, and then baked at 115 °C for 2 min, resulting in a high-quality film in each case. Compounds 1 and 2 exhibited poor adhesion to the primed wafer. Although they could be coated effectively onto an unprimed wafer, this resulted in almost complete lift-off during development. These two samples were discounted from further evaluation. The characteristic contrast curves of the remaining samples were evaluated on an HTG contact aligner, and the sensitivity and contrast for each sample is summarized in Figure 3.

As shown in Figure 3, the clearing dose for each system (i.e., the sensitivity) decreases with increased functionalization with DNQ side groups. To probe the differences on side-group architecture and reactivity, we synthesized a resist sample in which −5 DNQ, rather than −4 DNQ, was used as the side group. Comparison of the contrast curves for the 100%-protected compound reveals that at 405 nm, the −4-substituted DNQ has far higher sensitivity than the −5-substituted, requiring a clearing dose of 17.8 mJ/cm^2 compared to 212 mJ/cm^2 (Figure 4).

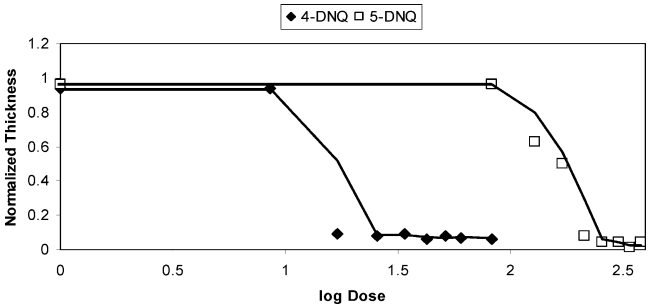

Figure 4. Comparison of −4 and −5 DNQ side groups. Note the higher sensitivity and contrast of the −4 DNQ-substituted analogue compared to the −5 DNQ-substituted analogue.

It has been previously noted that −4 DNQ is far more reactive than −5 DNQ, because it has a higher electron density at the diazo group.[38] Contrast was also far higher for the −4-substituted sample compared to the −5-substituted sample (Figure 4). Similar results have been noted with other DNQ ester dissolution inhibitors when blended with a base-soluble calixarene photoresist.[36] It is thought that the Wolff rearrangement of the −5-substituted species results in a moiety that is hydrolytically stable; therefore, the formation of the −5-substituted indene carboxylic acid is the final step in the process. The −4-substituted species undergoes the same Wolff rearrangement, although the ester formed in this case is hydrolytically unstable and undergoes further reaction, releasing a phenol group and a sulfonic acid group in the process. This leads to a higher concentration of base-soluble groups, resulting in a faster rate of dissolution in the exposed areas and therefore higher contrast.

DNQ-CR as a Resist for E-Beam Lithography. After demonstrating that DNQ-CR acts as a positive tone resist in optical lithography, we decided to examine its characteristics as a resist for e-beam lithography, another commonly used next-generation lithographic technique considered a good indicator of EUV performance. Compounds 8 and 4 were used in this investigation, as 8 exhibited the highest sensitivity and contrast in initial lithographic evaluation and compound 4 enabled us to examine how resolution varies with functionalization. After exposure and development, no images were observed. However, if the entire wafer was flood-exposed with UV radiation (365 nm) for 2 min after e-beam exposure and then developed in 0.26N TMAH, negative tone images were observed as opposed to the positive tone images obtained with optical lithography (Figure 5).

Interestingly, the minimum resolution achievable was dependent on the degree of functionalization of DNQ. For example, compound 4, functionalized with 50% DNQ, allowed the formation of features down to 150 nm (Figure 5A) at a dose of 600 $\mu C/cm^2$, but features smaller than this

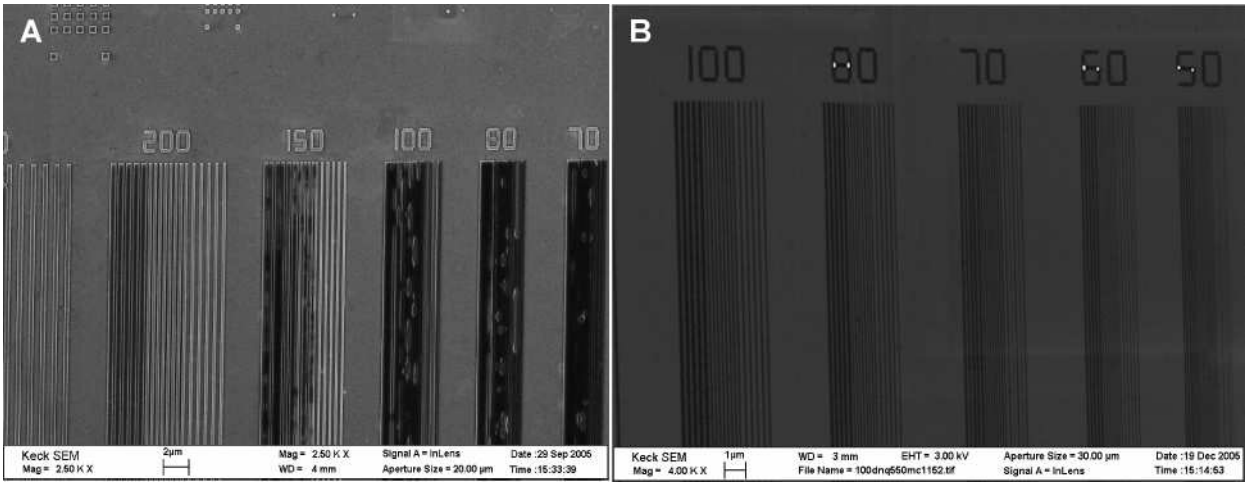

Figure 5. Negative tone images obtained after exposure of DNQ-CR resists with electron-beam radiation. These images were developed by flood exposing the e-beam-imaged resists with 366 nm UV radiation for 2 min followed by immersion in 0.26N TMAH. (A) Compound 4, 50% functionalized, is capable of resolving features down to 150 nm (dosage 600 μC/cm^2), although some pattern collapse is observed with 1:1 aspect ratio lines features. (B) Compound 8, 100% functionalized, is shown here resolving images as low as 50 nm at the same dosage.

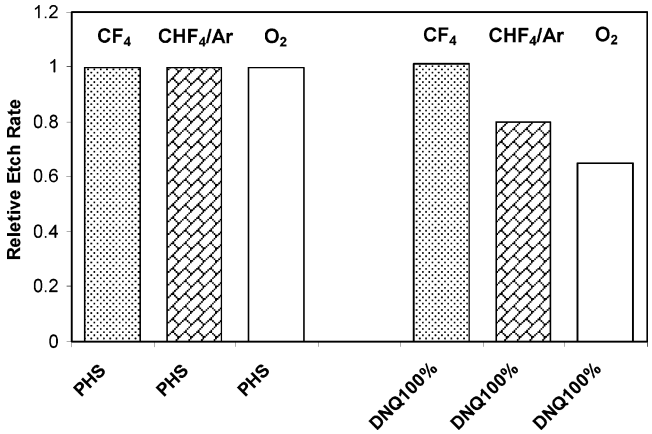

Figure 6. Etch resistance of DNQ-CR with reference to poly(hydroxyl styrene) to O_2, CF_4, and CHF_3/Ar etchants.

suffered from pattern collapse. Those samples with high degrees of functionalization (100%) enabled the formation of features as small as 60 nm (Figure 5B). Clearly, exposure to e-beam radiation results in the formation of a species less soluble in the developer compared to the indene carboxylic acid formed after the resist undergoes the Wolff rearrangement. A potential mechanism for this has been postulated by Pacansky and co-workers,[39] who examined the transformation that occurs when DNQ is blended with novaloc resin and exposed to e-beam radiation. The first step is loss of the diazo group to give a carbene, which when excited further by e-beam radiation reacts with the CH and CC bonds in aromatic groups on adjacent resist molecules to produce a substituted napthol, as outlined in Scheme 2.

A further point of interest is that when discrete DNQ molecules are used as dissolution inhibitors in e-beam or X-ray lithography,[39,40] a positive tone image is usually observed, as the product described in Scheme 2 could still be expected to show reasonable solubility in aqueous base. Our system, however, is rendered completely insoluble in the developer. We hypothesize that the reason for this is that

Scheme 2. Proposed Formation of a Cross-Lnked Network of DNQ after Exposure to E-Beam Radiation; A Substituted Napthol is Formed, Rather than the Indene Carboxylic Acid Formed after Exposure to UV Radiation, Which Results in Negative Tone Images as Opposed to Positive Tone Behavior (diagram adapted from Pacansky et al.[39])

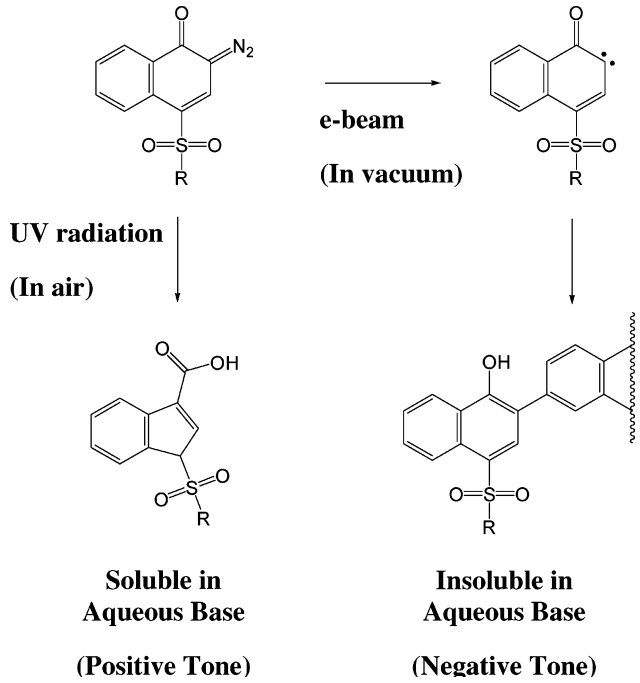

in our system, a high degree of cross-linking results in a species with a high molecular weight, in comparison to cross-linking discrete DNQ molecules, which results in smaller species with higher base solubility. In our samples with lower degrees of functionalization (i.e., 50%), a lower degree of cross-linking might be expected to result after exposure. In those samples with high degrees of functionalization, high degrees of cross-linking result in a high-molecular-weight insoluble resin, hence higher resolution.

Etch Resistance. Intuitively, it may be expected that small molecules are less etch resistant compared to polymer resists. As reactive ion etching is an important process used to transfer the pattern into an underlying hard substrate, the

(39) Pacansky, J.; Waltman, R. J. *J. Phys. Chem.* **1988**, *92*, 4558.
(40) Seeger, D. *IBM J. Res. Dev.* **1993**, *37*, 435.

etch resistance of these compounds was measured against O_2, CF_4, and CHF_3/Ar plasma ion etchants. All of these represent industry standard processes. Etch resistance was measured with reference to poly(hydroxyl styrene) (PHS). The results are shown in Figure 6. Compared to PHS, the resist shows comparable etch resistance to CF_4 and CHF_3/Ar plasmas, but is less resistant to O_2 plasma. It should be pointed out that these tests were conducted on unexposed DNQ-CR, rather than the cross-linked analogue suspected to result after exposure to electron-beam radiation. This might be expected to increase etch resistance, leading to results more comparable to the standard PHS.

Conclusions

In this submission, we have reported the synthesis and lithographic characterization of the first nonchemically amplified, DNQ-functionalized molecular glass resist for high-resolution lithography. The resist was synthesized via a simple base-catalyzed substitution reaction between a phenolic core and sulfonyl-chloride-modified DNQ. A series of DNQ-functionalized molecular glasses were characterized using FTIR and PXRD and found to undergo the Wolff rearrangement, resulting in the formation of positive tone images after exposure to 405 nm UV radiation. Exposure to e-beam radiation resulted in cross-linking, which led to the formation of negative tone images, and the minimum resolution of the features obtained was dependent on the degree of functionalization of DNQ. A high degree of DNQ functionalization resulted in smaller features. We believe this is due to higher degrees of cross-linking in the exposed resists. To perform as a commercially useful resist, we must dramatically increase the sensitivity of such resists. However, we believe that resists of this type, which combine the advantages of molecular glass resists with nonchemically amplified solubility switches, will prove to be the breakthrough that avoids the low-resolution limit of chemically amplified resists. We hope that this submission stimulates research into this emerging field to enable the emergence of truly next-generation resists.

Acknowledgment. We thank Intel Corporation for making this work possible through financial support. We also gratefully acknowledge the Cornell Nanoscale Science and Technology Facility (CNF) and the Cornell Center for Materials Research (CCMR) for use of their facilities and technical support.

CM062967T